

Title	Factor Graph-based Technique for Trajectory Tracking of Target with High Mobility
Author(s)	Jiang, Lei; Keerativoranan, Nopphon; Matsumoto, Tad; Takada, Jun-ichi
Citation	IEICE Communications Express, 12(1): 1-4
Issue Date	2024-09-10
Type	Journal Article
Text version	publisher
URL	http://hdl.handle.net/10119/19341
Rights	Copyright (C) 2024 Institute of Electronics, Information and Communication Engineers (IEICE). This work is licensed under a Creative Commons Attribution Non Commercial, No Derivatives 4.0 International License (CC BY-NC-ND). [https://creativecommons.org/licenses/by-nc-nd/4.0/] Lei Jiang, Nopphon Keerativoranan, Tad Matsumoto, and Jun-ichi Takada, IEICE Communications Express, Vol.12, No.1, 1-4, https://doi.org/10.23919/comex.2024XBL0132
Description	



Factor Graph-based Technique for Trajectory Tracking of Target with High Mobility

Lei Jiang ^{1, a)}, Nopphon Keerativoranan ^{1, b)}, Tad Matsumoto ^{1, 2, c)}, and Jun-ichi Takada ^{1, d)}

Abstract This paper presents a trajectory tracking algorithm for high-mobility targets using an extended Kalman smoothing (EKS)-based factor graph (FG). Traditional tracking methods often face challenges in maintaining accuracy and computational efficiency when dealing with fast-moving objects. Leveraging the probabilistic framework of factor graphs and robust estimation of EKS, the algorithm enhances tracking precision for fast-moving objects. Extensive simulations across various motion models demonstrate improved accuracy and robustness. The results indicate that this method effectively addresses the limitations of conventional tracking algorithms, providing a promising solution for applications in aviation, autonomous vehicles, and other domains requiring high-mobility tracking.

Keywords: Factor graph (FG), extended Kalman smoothing (EKS), trajectory tracking, high mobility

Classification: Navigation, Guidance and Control Systems

1. Introduction

The ability to accurately track high mobility targets is critical in various wireless location-based services (LBSs), including aviation, autonomous vehicles, and telecommunications [1]. Effective tracking enhances operational efficiency, safety, and reliability, making it a significant area of research and development. However, the high mobility of targets in these applications poses unique challenges, such as rapid changes in motion and environmental conditions that can degrade tracking accuracy and reliability.

Traditional tracking methods, such as Kalman and particle filters, have been widely used for tracking applications [2]. Kalman filters offer optimal estimation for linear systems with Gaussian noise but struggle with non-linear dynamics and non-Gaussian noise. Particle filters provide a robust solution for non-linear and non-Gaussian problems but at a high computational cost. These methods often face difficulties in maintaining accuracy and computational efficiency when applied to high-mobility targets.

Recent advances have focused on integrating advanced filtering techniques with probabilistic models to enhance

tracking performance. Extended Kalman filters (EKF) [3] and unscented Kalman filters (UKF) [4] have been proposed to handle nonlinear systems more effectively. However, these methods require significant computational resources and may not be suitable for real-time applications involving fast-moving targets. Factor graphs (FG) have emerged as a powerful framework for probabilistic modeling, offering flexibility and robustness in representing complex relationships within tracking problems [5, 6]. The application of factor graphs in high-mobility tracking is still evolving with ongoing research exploring their potential benefits and limitations.

To address the limitations of conventional tracking algorithms, this paper proposes a novel trajectory tracking algorithm that leverages the strengths of extended Kalman smoothing (EKS) within an FG framework. Factor graphs provide a unified representation of the probabilistic dependencies between variables, allowing efficient inference and estimation. By integrating EKS, the proposed method smooths state estimates over time, reducing the impact of noise and improving tracking accuracy.

The proposed method, named the FG-EKS algorithm, operates by constructing an FG that represents the relationships between the target's states and observations. The extended Kalman smoother is then applied to this graph, iteratively refining the state estimates by incorporating information from both past and future approximations. This approach not only improves tracking accuracy, but also maintains computational efficiency, making it suitable for real-time applications in high-mobility scenarios.

2. System model

In this paper, a distributed sensor-based FG is proposed. Each sensor receives direction of arrival (DoA) measurements as inputs. Similar to [5], the trigonometric relationship between DoA and position output is represented by the following connecting function:

$$\tan \phi_i = \left(\frac{Y_i - y_t}{X_i - x_t} \right) + u_{i,t} \quad (1)$$

where ϕ_i denotes the DoA at i -th sensor, and (X_i, Y_i) , (x_t, y_t) are the position of the i -th sensor and the target at time t , respectively. It is assumed that the measurement noise follows the Gaussian distribution $u_{i,t} \sim \mathcal{N}(0, \sigma_\phi^2)$. The geolocation-based FG algorithm (FG-GE) is detailed in [5]. The output of FG-GE serves as the observation state in the tracking phase described in this paper.

¹ Department of Transdisciplinary Science and Engineering, Tokyo Institute of Technology, Japan

² IMT Atlantique, CNRS UMR 6285, Lab-STICC, Brest, France, JAIST and University of Oulu (Emeritus)

a) jiang.l.ad@m.titech.ac.jp

b) nopphon.keerativoranan@ap.ide.titech.ac.jp

c) matumoto@jaist.ac.jp

d) takada@tse.ens.titech.ac.jp



In the tracking system, a non-linear discrete state-space model (SSM) is introduced to describe the real trajectory. The current state representing the target location is denoted as $\mathbf{s}(t) = [x_t, y_t]^T$ at the time step t ($t = \{1, 2, \dots, T\}$). The SSM is formulated as follows:

$$\mathbf{s}_t = f(\mathbf{s}_{t-1}) + \mathbf{e}_t \quad (2)$$

where $f(\cdot)$ is the non-linear function that connects two adjacent states, and $\mathbf{e}_t = [e_{x,t}, e_{y,t}]^T$ is the noise vector of the current position state. Similar to [5], the first-order Taylor series is used to linearize the function $f(\cdot)$, resulting in the expression:

$$\mathbf{s}_t \approx \mathbf{s}_{t-1} + \mathbf{v}_{t-1} + \mathbf{e}_t \quad (3)$$

where \mathbf{v}_{t-1} is the previous velocity state, defined as:

$$\mathbf{v}_{t-1} = \mathbf{v}_{t-2} + \mathbf{a}_{t-1} \quad (4)$$

where \mathbf{a}_{t-1} denotes the acceleration component. It should be noted that the relative time is normalized as $\Delta t = 1$ in this paper.

3. EKS-based Factor graph

The tracking phase consists of two passes: forward pass (filtering) and backward pass (smoothing). In the forward pass, the prediction state is obtained by maximizing the posterior probability of states and observations up to time t , given by:

$$p(\mathbf{s}_t, \mathbf{v}_t, \mathbf{a}_t | \mathbf{j}_{1:t}) = \sum_{\sim \mathbf{s}_t, \sim \mathbf{v}_t, \sim \mathbf{a}_t} p(\mathbf{s}_{1:t}, \mathbf{v}_{1:t}, \mathbf{a}_{1:t} | \mathbf{j}_{1:t}) \quad (5)$$

where \sim denotes the exclusion operation, and the subscript $\{1:t\}$ denotes the time series. $\mathbf{j}_{1:t}$ is the observation state. Similar to [5], using the Bayes theorem, Eq. (5) can be expressed as

$$\begin{aligned} & p(\mathbf{s}_{1:t}, \mathbf{v}_{1:t}, \mathbf{a}_{1:t} | \mathbf{j}_{1:t}) \\ & \propto \prod_{1:t} p(\mathbf{s}_t | \mathbf{s}_{t-1}, \mathbf{v}_{t-1}) p(\mathbf{v}_t | \mathbf{v}_{t-1}, \mathbf{a}_{t-1}) p(\mathbf{a}_t | \mathbf{a}_{t-1}) p(\mathbf{j}_t | \mathbf{s}_t) \end{aligned} \quad (6)$$

where \prod denotes iteration steps from 1 to t .

In the backward pass, the state in the current time step t can be updated using the state in the next time step $t+1$. Therefore, we are interested in updating the state at time t using the state at time $t+1$, given by:

$$\begin{aligned} & p(\mathbf{s}_{t-1} | \mathbf{s}_t, \mathbf{v}_t, \mathbf{a}_t, \mathbf{j}_{1:t+1}) \\ & \propto p(\mathbf{j}_{t+1} | \mathbf{s}_{t-1}, \mathbf{v}_{t-1}, \mathbf{a}_{t-1}, \mathbf{j}_{1:t}) p(\mathbf{s}_{t-1}, \mathbf{v}_{t-1}, \mathbf{a}_{t-1}, \mathbf{j}_{1:t}). \end{aligned} \quad (7)$$

Since \mathbf{j}_{t+1} depends only on \mathbf{s}_{t+1} , $p(\mathbf{j}_{t+1} | \mathbf{s}_{t-1}, \mathbf{v}_{t-1}, \mathbf{a}_{t-1}, \mathbf{j}_{1:t})$ can be expressed as:

$$p(\mathbf{j}_{t+1} | \mathbf{s}_{t-1}, \mathbf{v}_{t-1}, \mathbf{a}_{t-1}, \mathbf{j}_{1:t}) = p(\mathbf{j}_{t+1} | \mathbf{s}_{t+1}). \quad (8)$$

Therefore, the joint probability can be decomposed as:

$$\begin{aligned} & p(\mathbf{s}_{t-1}, \mathbf{v}_{t-1}, \mathbf{a}_{t-1}, \mathbf{j}_{1:t}) \\ & = p(\mathbf{s}_{t-1} | \mathbf{s}_t, \mathbf{v}_t) p(\mathbf{v}_{t-1} | \mathbf{v}_t, \mathbf{a}_t) p(\mathbf{a}_{t-1} | \mathbf{a}_t) p(\mathbf{s}_t, \mathbf{v}_t, \mathbf{a}_t, \mathbf{j}_{1:t}). \end{aligned} \quad (9)$$

Combining Eq. (7) through Eq. (9), the posterior probability using future state information can be expressed as:

$$\begin{aligned} & p(\mathbf{s}_{t-1}, \mathbf{v}_{t-1}, \mathbf{a}_{t-1} | \mathbf{j}_{1:t+1}) \\ & \propto p(\mathbf{j}_{t+1} | \mathbf{s}_{t+1}) p(\mathbf{s}_{t-1} | \mathbf{s}_t, \mathbf{v}_t) p(\mathbf{v}_{t-1} | \mathbf{v}_t, \mathbf{a}_t) p(\mathbf{a}_{t-1} | \mathbf{a}_t). \end{aligned} \quad (10)$$

Based on the recursive form of the posterior probability in both the forward pass and backward pass, the FG can be constructed, as depicted in Fig. 1. The entire FG-EKS tracking system can be divided into 5 steps.

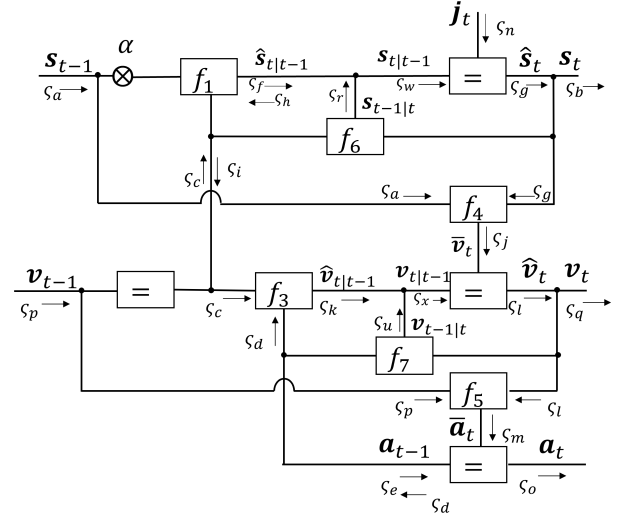


Fig. 1 FG-EKS for tracking system

• Step 1: Forward pass prediction

The forward pass prediction $\hat{\mathbf{s}}_t | t-1$ is calculated based on the previous state \mathbf{s}_{t-1} . The corresponding message flow ζ_f is given by:

$$\begin{aligned} & \zeta_f(\hat{\mathbf{s}}_t | t-1) \\ & = \sum_{\mathbf{s}_{t-1}} \sum_{\hat{\mathbf{v}}_{t-1}} f_1(\mathbf{s}_t | \mathbf{s}_{t-1}, \hat{\mathbf{v}}_{t-1}) \zeta_a(\mathbf{s}_{t-1}) \zeta_c(\hat{\mathbf{v}}_{t-1}) \end{aligned} \quad (11)$$

where $\zeta_a(\mathbf{s}_{t-1})$ and $\zeta_c(\hat{\mathbf{v}}_{t-1})$ represent the message flows of the previous position state and velocity state, respectively. The state prediction function $f_1(\mathbf{s}_t | \mathbf{s}_{t-1}, \hat{\mathbf{v}}_{t-1})$ is given by:

$$f_1(\mathbf{s}_t | \mathbf{s}_{t-1}, \hat{\mathbf{v}}_{t-1}) = \alpha \cdot \mathbf{s}_{t-1} + \hat{\mathbf{v}}_{t-1} \quad (12)$$

where α is the forgetting factor used to balance the weight between position state and velocity state. This adjustment is necessary in high mobility tracking scenarios due to the significant distance changes between consecutive time steps caused by the fast speed of the target.

• Step 2: Forward state update

The estimated current state $\hat{\mathbf{s}}_t$ is refined using the observation state \mathbf{j}_t to update the forward pass prediction $\hat{\mathbf{s}}_t | t-1$

$$\zeta_g(\hat{\mathbf{s}}_t) = \zeta_f(\hat{\mathbf{s}}_t | t-1) \zeta_n(\mathbf{j}_t). \quad (13)$$

• Step 3: Backward state smoothing

In this step, the updated forward state $\hat{\mathbf{s}}_t$ serves as an approximate future message to smooth the backward state $\mathbf{s}_{t-1} | t$

$$\zeta_r(\mathbf{s}_{t-1} | t) = \sum_{\mathbf{s}_t} \sum_{\hat{\mathbf{v}}_{t-1}} f_6(\mathbf{s}_{t-1} | t | \mathbf{s}_t, \hat{\mathbf{v}}_{t-1}) \zeta_g(\mathbf{s}_t) \zeta_c(\hat{\mathbf{v}}_{t-1}) \quad (14)$$

where backward pass function $f_6(\mathbf{s}_{t-1|t}|\mathbf{s}_t, \hat{\mathbf{v}}_{t-1})$ is given by

$$f_6(\mathbf{s}_{t-1|t}|\mathbf{s}_t, \hat{\mathbf{v}}_{t-1}) = \mathbf{s}_t - \hat{\mathbf{v}}_{t-1}. \quad (15)$$

It should be noted that, compared with the conventional off-line Kalman smoothing method, the proposed FG-EKS only uses the approximated current state as future message to estimate the previous state. Hence, the real-time processing is possible through FG-EKS.

- Step 4: Prediction Refinement

The smoothed backward state $\mathbf{s}_{t-1|t}$ is further combined with the filtered forward state to refine the prediction state $\hat{\mathbf{s}}_{t|t-1}$ to estimate the current state \mathbf{s}_t , given by:

$$\zeta_w(\hat{\mathbf{s}}_{t|t-1}) = \prod \zeta_r(\mathbf{s}_{t-1|t})\zeta_f(\mathbf{s}_{t|t-1}), \quad (16)$$

$$\zeta_g(\mathbf{s}_t) = \zeta_f(\mathbf{s}_{t|t-1})\zeta_n(\mathbf{j}_t). \quad (17)$$

Note that same as in position state, the forward pass update and backward pass update can be also applied to velocity state.

- Step 5: Gradient update

Since the prediction state of velocity $\hat{\mathbf{v}}_{t|t-1}$ is updated and refined as that in position state, we focus on the two gradient vector updates \mathbf{v}_t and \mathbf{a}_t in this step. The velocity can be updated using a correction term $\hat{\mathbf{v}}_t$ to refine the predicted velocity $\mathbf{v}_{t|t-1}$ that is refined by the forward pass update $\hat{\mathbf{v}}_{t-1}$ and the backward pass update $\mathbf{v}_{t-1|t}$. The current velocity \mathbf{v}_t is given by:

$$\zeta_l(\mathbf{v}_t) = \zeta_j(\hat{\mathbf{v}}_t)\zeta_k(\mathbf{v}_{t|t-1}) \quad (18)$$

where the message flow $\zeta_j(\hat{\mathbf{v}}_t)$ is calculated from the state difference between two adjacent positions, given by:

$$\zeta_j(\hat{\mathbf{v}}_t) = \sum_{\mathbf{s}_{t-1}} \sum_{\mathbf{s}_t} f_4(\hat{\mathbf{v}}_t|\mathbf{s}_t, \mathbf{s}_{t-1})\zeta_a(\mathbf{s}_{t-1})\zeta_g(\mathbf{s}_t) \quad (19)$$

where the state difference function $f_4(\hat{\mathbf{v}}_t|\mathbf{s}_t, \mathbf{s}_{t-1})$ is given by:

$$f_4(\hat{\mathbf{v}}_t|\mathbf{s}_t, \mathbf{s}_{t-1}) = \mathbf{s}_t - \mathbf{s}_{t-1} \quad (20)$$

The forward pass prediction state $\zeta_k(\mathbf{v}_{t|t-1})$ is achieved by combining the previous velocity state and acceleration component, given by:

$$\begin{aligned} \zeta_k(\hat{\mathbf{v}}_{t|t-1}) &= \sum_{\mathbf{v}_{t-1}} \sum_{\mathbf{a}_{t-1}} f_3(\hat{\mathbf{v}}_{t|t-1}|\mathbf{v}_{t-1}, \mathbf{a}_{t-1})\zeta_c(\mathbf{v}_{t-1})\zeta_d(\mathbf{a}_{t-1}) \end{aligned} \quad (21)$$

where the function $f_3(\hat{\mathbf{v}}_{t|t-1}|\mathbf{v}_{t-1}, \mathbf{a}_{t-1})$ is given by:

$$f_3(\mathbf{v}_{t|t-1}|\mathbf{v}_{t-1}, \mathbf{a}_{t-1}) = \hat{\mathbf{v}}_{t-1} + \mathbf{a}_{t-1} \quad (22)$$

Similarly as in updating the velocity state, a correction term $\hat{\mathbf{a}}_t$ is introduced to update the acceleration. Using two adjacent velocity, the acceleration is given by:

$$\zeta_m(\hat{\mathbf{a}}_t) = \sum_{\mathbf{v}_{t-1}} \sum_{\mathbf{v}_t} f_5(\hat{\mathbf{a}}_t)\zeta_c(\mathbf{v}_{t-1})\zeta_l(\mathbf{v}_t) \quad (23)$$

where the function $f_5(\hat{\mathbf{a}}_t)$ is given by:

$$f_5(\hat{\mathbf{a}}_t) = \mathbf{v}_t - \mathbf{v}_{t-1} \quad (24)$$

Thereby, the updated acceleration is given by:

$$\zeta_o(\mathbf{a}_t) = \zeta_c(\mathbf{a}_{t-1})\zeta_m(\hat{\mathbf{a}}_t) \quad (25)$$

4. Simulation results

To assess the robustness of the proposed FG-EKS technique, several outdoor trajectory models of a small commercial UAV are employed. The positions of three sensors are distributed as follows: $(X_1, Y_1) = (0, 0)$ m, $(X_2, Y_2) = (70, 12)$ m, $(X_3, Y_3) = (-60, 81)$ m. The relative time between two states is normalized as $\Delta t = 1$.

4.1 Constant velocity (CV) model

The constant velocity (CV) model assumes that the UAV's velocity remains unchanged over time, resulting in linear changes in its position. The CV trajectory is described by:

$$\begin{aligned} y_t &= y_{t-1} + v_y + \varepsilon_y \\ x_t &= x_{t-1} + v_x + \varepsilon_x \end{aligned} \quad (26)$$

where v_x and v_y denote the speed on the x-axis and the y-axis, respectively. Small consumer UAVs typically operate at speeds ranging from 15 to 50 km/h (approximately 4.17 to 13.89 m/s). Here, $v_y = v_x = 10$ m/s. $\varepsilon = [\varepsilon_y, \varepsilon_x]^T$ represents the random trajectory deviation from the ideal path, assumed to follow a Gaussian distribution $\varepsilon \sim (0, \sigma^2)$. Let $\sigma = 0.5$ m to account for the trajectory perturbations. The time step t is set within $t = \{1, \dots, 25\}$ s. The tracking performance is illustrated in Fig. 2. Clearly, the proposed FG-EKS can achieve higher accuracy in trajectory tracking compared to FG-EKF, as indicated by the average root mean square error (RMSE).

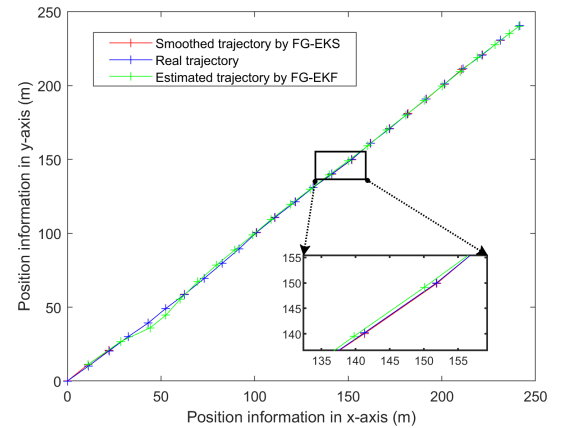


Fig. 2 Trajectory tracking of CV model

4.2 Constant acceleration (CA) model

In a CA model, the velocity of the UAV changes at a constant rate over time, resulting in linear equations for position and velocity updates. The CA model is defined as

$$\begin{aligned} y_t &= y_{t-1} + v_{y,t} + \varepsilon_y \\ x_t &= x_{t-1} + v_{x,t} + \varepsilon_x \end{aligned} \quad (27)$$

where

$$\begin{aligned} v_{y,t} &= v_{y,t-1} + a_y \\ v_{x,t} &= v_{x,t-1} + a_x \end{aligned} \quad (28)$$

Here, $\mathbf{a} = [a_y, a_x]^T$ is the acceleration component. Let $a_y = a_x = 0.1\text{m/s}^2$, and the initial speeds $v_{y,0} = v_{x,0} = 0.1\text{m/s}$.

As shown in Fig. 3, the proposed technique accurately tracks the trajectory of the CA model, even as the speed increases.

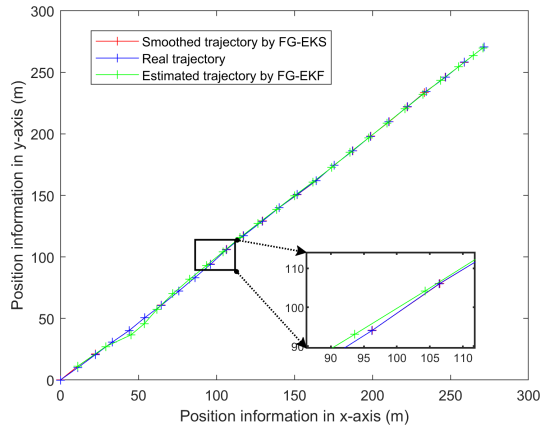


Fig. 3 Trajectory tracking of CA model

4.3 Constant turn rate and velocity (CTRV) model

The CTRV model describes the motion of the UAV, where it maintains a constant speed while executing turns at a constant rate. The CTRV model is defined as

$$\mathbf{s}_t = \mathbf{s}_{t-1} + \mathbf{v}_t + \mathbf{u} \quad (29)$$

where the velocity \mathbf{v}_t is given by:

$$\mathbf{v}_t = \begin{bmatrix} \cos(\theta_t) \\ \sin(\theta_t) \end{bmatrix} \cdot \|\mathbf{v}_{t-1}\| \quad (30)$$

where θ_t is heading angle, given by:

$$\theta_t = \theta_{t-1} + \omega \quad (31)$$

Here, ω denotes the constant turn rate. Let the turn rate $\omega = \frac{\pi}{180}$ rad/s and the initial heading angle $\theta_0 = \frac{\pi}{10}$ rad. The results are depicted in Fig. 4. Compared to CV and CA models, the tracking accuracy of the proposed technique is initially affected by nonlinear motion. However, the performance improves over time as the iterative process in the factor graph suppresses the prediction errors.

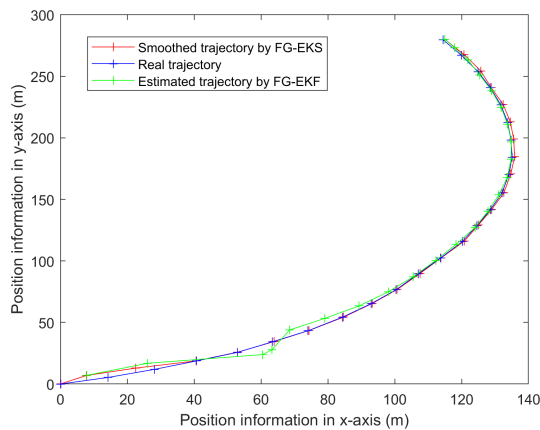


Fig. 4 Trajectory tracking of CTRV model

The tracking accuracy of the proposed technique is further evaluated by calculating the average root mean square

error across varying direction of arrival (DoA) measurement errors. The results are summarized in Table. I, where it is evident that the proposed FG-EKS achieves superior performance across different models, demonstrating its high robustness.

Table I Average root mean square error (m) of tracking vs. standard deviation of DOA

	σ_ϕ (°)	1	5	15	20	25
CV	EKS	0.15	0.51	1.32	3.58	8.56
	EKF	0.47	1.56	3.78	8.99	17.11
CA	EKS	0.18	0.63	1.45	4.13	12.36
	EKF	0.83	1.75	4.15	11.46	20.78
CTRV	EKS	0.66	1.55	4.46	9.89	15.20
	EKF	1.40	3.46	8.85	16.66	28.92

5. Conclusion

In this paper, we have proposed a novel trajectory tracking algorithm for high-mobility targets using an EKS-based FG. This approach addresses limitations of traditional tracking methods by leveraging EKS's robust estimation capabilities within a probabilistic FG framework. We have evaluated our method through extensive simulations of various motion models, including CV, CA, and CTRV. The results demonstrate that the FG-EKS algorithm significantly improves tracking accuracy and robustness. The results highlight the method's effectiveness in mitigating prediction errors associated with nonlinear and high-speed trajectories, making it a promising solution for diverse applications.

References

- [1] M. Yassin and E. Rachid, "A survey of positioning techniques and location based services in wireless networks," *2015 IEEE International Conference on Signal Processing, Informatics, Communication and Energy Systems (SPICES)*, Kozhikode, India, 2015, pp. 1-5. DOI: [10.1109/SPICES.2015.7091420](https://doi.org/10.1109/SPICES.2015.7091420)
- [2] Q. Li, R. Li, K. Ji and W. Dai, "Kalman Filter and Its Application," *2015 8th International Conference on Intelligent Networks and Intelligent Systems (ICINIS)*, Tianjin, China, 2015, pp. 74-77. DOI: [10.1109/ICINIS.2015.35](https://doi.org/10.1109/ICINIS.2015.35)
- [3] G. A. Einicke and L. B. White, "Robust extended Kalman filtering," in *IEEE Transactions on Signal Processing*, vol. 47, no. 9, pp. 2596-2599, Sept. 1999. DOI: [10.1109/78.782219](https://doi.org/10.1109/78.782219)
- [4] E. A. Wan and R. Van Der Merwe, "The unscented Kalman filter for nonlinear estimation," *Proceedings of the IEEE 2000 Adaptive Systems for Signal Processing, Communications, and Control Symposium (Cat. No.00EX373)*, Lake Louise, AB, Canada, 2000, pp. 153-158. DOI: [10.1109/ASSPCC.2000.882463](https://doi.org/10.1109/ASSPCC.2000.882463)
- [5] L. Jiang, M. Cheng and T. Matsumoto, "A TOA-DoA Hybrid Factor Graph-based Technique for Multi-target Geolocation and Tracking," *IEEE Access*, vol. 9, pp. 14203-14215, 2021. DOI: [10.1109/ACCESS.2021.3052233](https://doi.org/10.1109/ACCESS.2021.3052233)
- [6] M. Cheng, M. R. K. Aziz and T. Matsumoto, "Integrated Factor Graph Algorithm for DOA-Based Geolocation and Tracking," *IEEE Access*, vol. 8, pp. 49989-49998, 2020. DOI: [10.1109/ACCESS.2020.2979510](https://doi.org/10.1109/ACCESS.2020.2979510)